JOURNAL OF MATERIALS SCIENCE 12 (1977) 28–34

Pyramidal yield criteria for epoxides

A. S. WRONSKI, M. PICK*
School of Materials Science, University of Bradford, West Yorkshire, UK

The tensile, compressive and shear yield strengths of two epoxides were measured under superposed hydrostatic pressure extending to 300 MN m^{-2}. For both materials, the ratio of the moduli of the tensile, σ_T, to compressive, σ_C, yield stress at atmospheric pressure was approximately 3:4, as has been reported previously for a number of thermoplastics. The $\sigma_2 = \sigma_3$ envelope in stress space was plotted according to these two-parameter (σ_C and σ_T) yield criteria: conical, paraboloidal and pyramidal; the best correlation was with the last. The experimental tensile and compressive data for tests under pressure, however, fit slightly better two straight lines which are consistent with a three-parameter single hexagonal pyramidal yield surface. For plane stress and shear under pressure yield envelopes of these surfaces, the correlation with experimental data is again best for the pyramidal criteria, except for biaxial or triaxial tension when these resins are brittle. The third independent parameter employed in the pyramidal criterion was the equi-biaxial compressive yield stress, determined by tensile experiments under appropriate superposed hydrostatic pressure; alternatively plane strain compressive yield stress, σ_{PC}, may be used.

1. Introduction

It is generally recognized that neither the one-parameter Huber–von Mises [1, 2] or Tresca [3] criterion describes the macroscopic yielding behaviour of polymers [4] and accordingly several hydrostatic pressure-dependent two-parameter models [5–15] have been proposed, all based on the criterion postulated for soils by Coulomb [16] and subsequently theoretically developed [17–23]. In general the criteria have been compared with experiments on thermoplastics tested in tensile, compressive or shear mode under confining pressure. All the criteria correctly show that the uniaxial tensile, σ_T, and compressive, σ_C, yield stresses are unequal, and in fact two-parameter theories can be expressed in terms of these two parameters. Several studies, however, do not report the experimental values of σ_T and σ_C.

Fairly recently, Caddell *et al.* [11] reviewed some of the data on yielding of polymers under biaxial and triaxial loading in terms of the proposals of Sternstein and Ongchin [9] and Raghava *et al.* [14]. They dismissed in their *Introduction* the Mohr–Coulomb [15] model, much favoured in soil mechanics and in an earlier review of the yield behaviour of polymers by Ward [4]. Paul [22], however, when considering macroscopic criteria for flow in solids, suggested that to overcome the limitation of the independence of the Mohr–Coulomb criterion on the intermediate principal stress, σ_2, a third material parameter in addition to σ_T and σ_C needs be considered, and proposed a generalized pyramidal failure surface:

$$X\sigma_1 + Y\sigma_2 + Z\sigma_3 = 1, \tag{1}$$

where σ_1 and σ_3 are the maximum and minimum principal stresses. The simplest surface of this type is a single hexagonal pyramid; for the Mohr–Coulomb pyramid $Y = 0$. For given values of σ_T and σ_C, there is only one two-parameter pyramid and geometrically it relates equally to the Mohr–Coulomb [4, 15] and "modified Tresca" [24] criteria, which differ in their theoretical derivations [23, 24].

Very recently, Li and Wu [23] re-examined the problem of pressure and normal stress effects in shear yielding and, differentiating between these, also concluded that a three-parameter theory is the

* Present address: Department of Metallurgy, University of Cambridge, UK.

most general for polyhedral yield surfaces. Their three material constants, α, β, and τ_0 refer to the condition for yielding:

$$|\tau| + \alpha\sigma_N + \beta\sigma_H \geqslant \tau_0 \tag{2}$$

where τ is the shear stress, σ_N the normal stress in the plane and σ_H the hydrostatic component of stress. In developing their model, Li and Wu [23] show that at the apex of the pyramid $\sigma_H = \sigma_V = \tau_0/(\alpha + \beta)$. This equi-triaxial tensile yield condition has been previously employed by Paul [22] to define the third parameter, in addition to σ_T and σ_C, of his single hexagonal pyramids:

$$\frac{\sigma_1}{\sigma_T} + \frac{\sigma_V\sigma_T + |\sigma_C|\,\sigma_T - |\sigma_C|\,\sigma_V}{|\sigma_C|\,\sigma_T\sigma_V}\sigma_2 - \frac{\sigma_3}{|\sigma_C|} = 1. \tag{3}$$

An additional problem with the formulation of yielding criteria in polymers is that there is no accepted definition of what constitutes yielding on the load–deflection curve determined at a given deformation rate. It would appear, however, that whatever the definition, the ratio of the uniaxial tensile to compressive yield stress for a given material is approximately the same: at least for the same type of material, different workers using different criteria report approximately the same ratios. It should be added that for a number of dissimilar polymers, as for the two resins which form the subject of this communication, $\sigma_T : \sigma_C$ evaluates to ≈ -0.75. Accordingly reduced stresses, P, will be employed and, as the tensile yield stress, σ_T, in brittle polymers need not be a physical parameter, stresses will be expressed in terms of $|\sigma_C|$, i.e. $P = \sigma/|\sigma_C|$. In our studies we define yielding to be taking place when the maximum load in a given deformation experiment is reached and our yield stresses are quoted in terms of the original cross-section, i.e. are nominal or engineering stresses. (In discussing this problem, Bowden [24], defined the intrinsic yield point to occur at the maximum true stress.) Different criteria predict different surfaces in stress space and, therefore, it is instructive to compare these and specific envelopes for given relationships of the three principal stresses, σ_1, σ_2 and σ_3. In this communication the convention that $\sigma_1 > \sigma_2 > \sigma_3$ is not adhered to when plotting figures, as only isotropic materials are considered.

2. Experimental procedure

The material for the investigation, in the form of 6 mm diameter rods, was kindly given by Dr D.C. Phillips of AERE, Harwell, who also provided data for pure shear yield at atmospheric pressure. The Ciba resin 1 consisted of 100 pbw MY750/80 pbw MNA/1 pbw BDMA and was cured for 2 h at 120° C and post-cured for 4 h at 180° C. Also reported are some new results on MY753/HY951, resin 2, previously studied by Dibb [25] and Wronski [26], to which reference will be made. For this epoxide the uniaxial tensile yield stress was 67 and compressive $-90\,\text{MN m}^{-2}$.

All tests were performed on an Hedeby universal tester fitted with a $0.3\,\text{GN m}^{-2}$ Coleraine pressure cell. Tensile specimens were cylindrical with ~ 10 mm gauge length and ~ 2 mm gauge diameter, compression specimens were cylinders 8 mm high and 5 mm diameter. Tests were carried out at a cross-head speed of $10^{-3}\,\text{mm sec}^{-1}$. Shear yield stress was measured by (double) shearing a solid cylinder, 4.7 mm diameter, between a rod and a near fitting tube in the high pressure apparatus [25]. The yield stress in pure shear so determined, $58\,\text{MN m}^{-2}$, agrees fairly well with Phillips' determined in torsion, $55\,\text{MN m}^{-2}$.

In the pressure experiments, the axial forces were measured externally to the pressure cell on a semiconductor load cell only, and therefore included the frictional forces at the pull and dummy rod seals of the yoke straining assembly. These frictional forces could only be measured (at the test pressure) prior to the straining of the specimen and after its failure (in tension or shear). These forces increased slightly or not at all during testing and, in general, interpolation could be used to determine them at yield. The reliability of this procedure was shown to be adequate when load on the specimen was simultaneously measured directly on an internal load cell incorporated for some tests on metals [27].

3. Results

Ten specimens of resin 1 were tested in uniaxial tension at atmospheric pressure and of these five showed a load maximum and failed soon afterwards and five failed as the load was rising after some 5% elongation. The nominal failure stresses for the latter group were in the range 69 to $88\,\text{MN m}^{-2}$ ($76 \pm 7\,\text{MN m}^{-2}$), whilst the yield stresses for the former were in the range 85 to $91\,\text{MN m}^{-2}$ ($88 \pm 3\,\text{MN m}^{-2}$) and their failure strains were slightly higher. (The behaviour of only the latter group we will consider as brittle, although the appearance of the failure surfaces was similar in all cases). Frac-

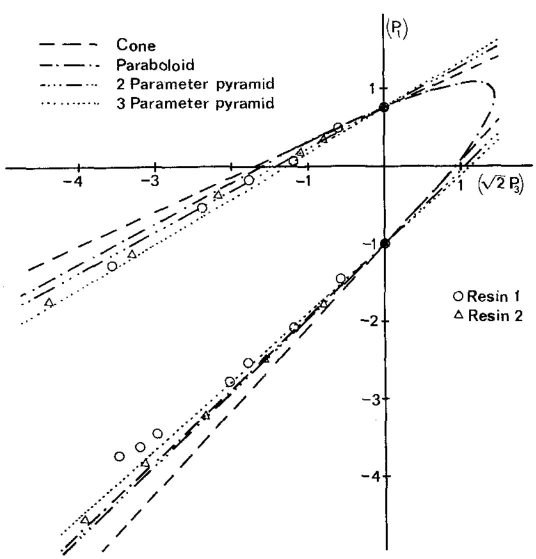

Figure 1 Yield strength data for tensile and compressive tests carried out under superposed hydrostatic pressure. Shown plotted are yield envelopes in $\sigma_2 = \sigma_3$, i.e. (0 1 1), plane of normalized stress space P_1, P_2, P_3, calculated according to the paraboloidal, conical and pyramidal two-parameter criteria. The two parameters were uniaxial compressive yield strength, equal to -1, and uniaxial tensile yield strength, equal to 0.75. Note that the two best fit straight lines (. . . . . .) are consistent with a three-parameter pyramidal yield surface.

ture at markedly lower stresses than expected for yielding was even more pronounced if biaxial or triaxial tension was applied, e.g. $\sigma_1 = 3.3\,\mathrm{MN\,m^{-2}}$, $\sigma_2 = \sigma_3 = 0.8\,\mathrm{MN\,m^{-2}}$. The average atmospheric σ_C for five specimens of resin 1 was found to be $-119 \pm 1\,\mathrm{MN\,m^{-2}}$. $\sigma_T : |\sigma_C|$ evaluates thus to 0.74.

The influence of superposed hydrostatic pressure, $-H$, was to suppress brittleness and increase failure strain, but only to some 8 to 10% for $50 > -H > 300\,\mathrm{MN\,m^{-2}}$. The tensile yield strength decreased with increasing pressure as the (maximum) shear stress at yield increased. The data (in terms of reduced stresses) relate to the upper plots of Fig. 1 for which σ_1 is the maximum principal stress (applied axial stress minus hydrostatic pressure $-H$) and $-\sigma_3(=-\sigma_2)$ the superposed hydrostatic pressure. It is seen that the pressure dependence of the tensile yield stress is approximately linear $(P_3 + P_2)/\sqrt{2} = \sqrt{2}P_3$ rather than P_3 is chosen as the abcissa for Fig. 1 because the experimental points refer to the $\sigma_2 = \sigma_3$, i.e. (0 1 1), plane of the P_1, P_2, P_3 stress space. It is to be noted that when $-H > 100\,\mathrm{MN\,m^{-2}}$, although a specimen was being extended, all the principal stresses at yield (and failure) were compressive.

There is also an approximately linear dependence of the compressive yield stress on hydrostatic pressure: data relating to the lower plots of Fig. 1. Please note that the maximum principal stress is now the hydrostatic pressure and P_1 $(= \sigma_1/|\sigma_C|)$ refers to the minimum principal stress in the direction of straining.

In Fig. 2, data are shown from shear experiments under pressure $(-\sigma_2)$. Each test provides two points for the yield surface as, for example, pure shear gives $\sigma_1 = \sigma_A$, $\sigma_2 = 0$, $\sigma_3 = -\sigma_A$ and $\sigma_1 = -\sigma_A$, $\sigma_2 = 0$, $\sigma_3 = \sigma_A$. The relevant plane in stress space is $(1\,\bar{2}\,1)$ and the perpendicular axes chosen for Fig. 2 are $(P_1 + P_2 + P_3)/\sqrt{3}$, i.e. [1 1 1], the hydrostatic line $P_1 = P_2 = P_3$, and $(P_1 - P_3)/\sqrt{2}$, i.e. $[1\,0\,\bar{1}]$: $P_1 = -P_3; P_2 = 0$.

Fracture surfaces of tensile specimens tested at atmospheric pressure showed surface flaw initiation sites and regions of slow growth and rapid propagation (e.g. Fig. 3). For tensile specimens tested under hydrostatic pressure all stresses are frequently compressive, yet cracking was observed (e.g. Figs. 4 and 5). This cracking was predominantly normal to the tensile axis, but failure

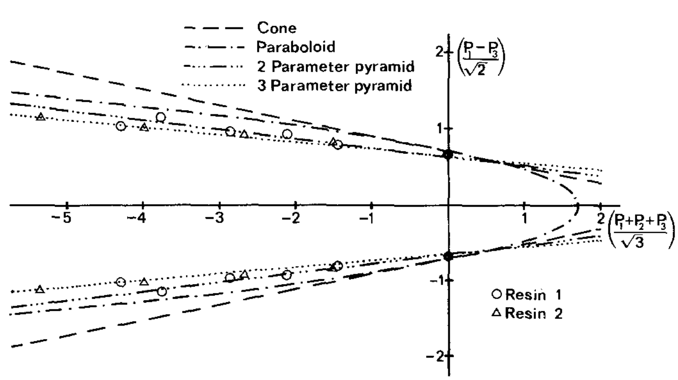

Figure 2 Yield strength data for shear tests carried out under superposed hydrostatic pressure. Shown plotted are yield envelopes in $\sigma_1 + \sigma_3 = 2\sigma_2$, i.e. $(1\,\bar{2}\,1)$, plane of normalized stress space P_1, P_2, P_3 calculated according to the paraboloidal, conical, and two- and three-parameter pyramidal criteria; the parameters being the same as for Fig. 1.

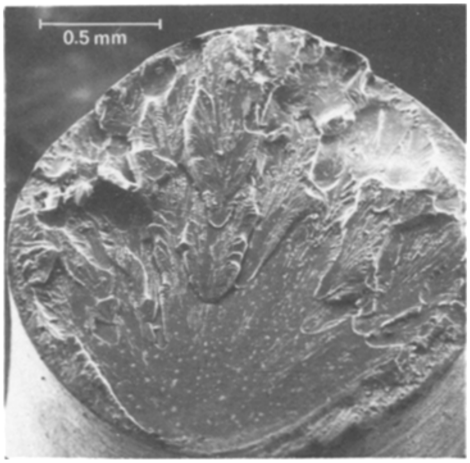

Figure 3 A scanning electron micrograph of the failure surface of a resin 1 specimen fractured in simple tension at atmospheric pressure. Note the surface initiation site and regions of slow growth and rapid crack propagation.

surfaces included surface lips, at approximately 45° to this axis. The failure initiation sites in these specimens were not always situated at the surface (e.g. Fig. 5) and the region of slow growth appeared to decrease in size with increasing pressure; note its absence in Fig. 4 relating to failure under superposed pressure of 300 MN m^{-2}.

Observation of tested tensile and compressive specimens between crossed polars failed to reveal regions of localized birefringence except in one specimen. This was under superposed hydrostatic pressure of 90 MN m^{-2}, i.e. nearly under conditions of equi-biaxial compression (specimen of Fig. 5). The shear bands appeared orthogonal and were at ~ 45° to the straining direction in close proximity to the failure surface (Fig. 5) on both pieces of the fractured specimen.

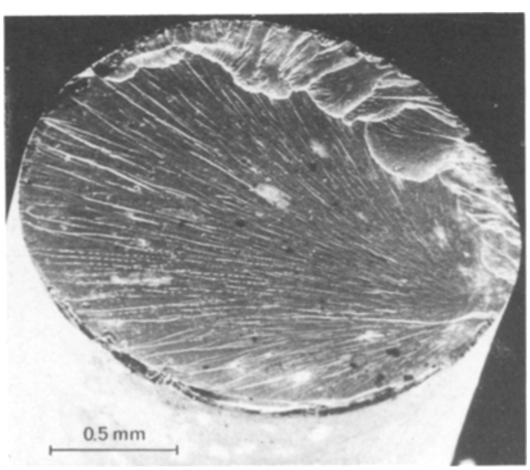

Figure 4 A scanning electron micrograph of the failure surface of a resin 1 specimen pulled under superposed hydrostatic pressure of 300 MN m^{-2}. Note the near-surface initiation site, region of fast crack growth and a large lip, approximately at 45° to the plane of the main failure surface.

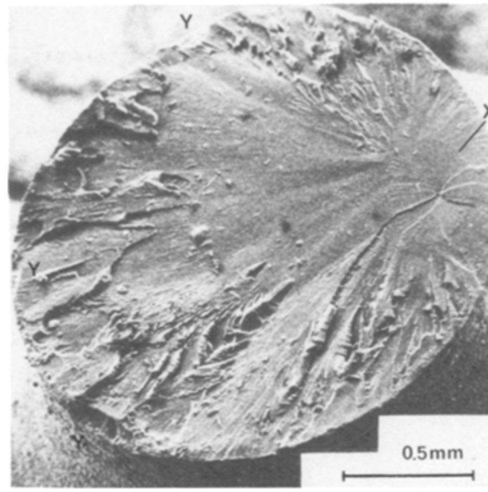

Figure 5 A scanning electron micrograph of the fracture surface of a resin 1 specimen which failed in (approximately) equi-biaxial compression. Note the internal failure initiation site surrounded by a disc-like zone of slow growth, X, the region of fast crack propagation and several small surface lips, Y, remote from the failure initiation site.

4. Discussion

Mechanical properties of thermosetting resins have not been studied as extensively as those of thermoplastics, but the similarities in their behaviours have been noted [4]. Bowden and Jukes [6, 12] have used the same types of analysis as those for thermoplastics and we will attempt to put our data in the context of previous work on polymers in general, starting with two-parameter models. Caddell *et al.* [14] showed the similarities in plane stress of the criteria they reviewed and drew attention to the necessity of measuring both σ_T and σ_C. These are the two independent parameters in terms of which we will present the three commonly postulated two-parameter criteria: $\tau_{oct} = \tau_0 - \mu\sigma_H$ [4, 12, 14] which can be rewritten as:

$$[(P_1 - P_2)^2 + (P_2 - P_3)^2 + (P_3 - P_1)^2]^{\frac{1}{2}} = \frac{2\sqrt{2}CT}{(C+T)} - (P_1 + P_2 + P_3)\frac{\sqrt{2}(C-T)}{(C+T)} \tag{4}$$

or

$$\left[\frac{2CT}{C-T}-\frac{P_1+P_2+P_3}{3}\right]^2$$

$$=\frac{3}{1+2(C-T/C+T)^2}\left[\left(\frac{2CT}{C-T}-P_1\right)^2+\left(\frac{2CT}{C-T}-P_2\right)^2+\left(\frac{2CT}{C-T}-P_3\right)^2\right], \quad (5)$$

i.e. a cone [9, 15, 17, 21]; the paraboloid [14, 18, 21]:

$$(P_1-P_2)^2+(P_2-P_3)^2+(P_3-P_1)^2 + 2(C-T)(P_1+P_2+P_3)=2CT; \ldots . \quad (6)$$

and the Mohr–Coulomb pyramid [4, 20, 22]:

$$\frac{P_1}{T}-\frac{P_3}{C}=1 \quad (7)$$

where τ_{oct} is the octahedral shear stress, τ_0 and μ are constants, σ_H is the hydrostatic component of stress (mean stress), P_1, P_2 and P_3 are reduced stresses (in terms of $|\sigma_C|$) and T and C are the moduli of the reduced tensile and compressive uniaxial yield stresses, i.e. $C \equiv 1$. A number of ways have been used to plot tensile and compressive strength data under superposed hydrostatic pressure, but only one [22], σ_1 versus $\sqrt{2}\sigma_2=\sqrt{2}\sigma_3$, i.e. yield locus in the plane $\sigma_2=\sigma_3$, brings out clearly the relevance and limitation of these triaxial tests to the yield surface determination. Accordingly, we have chosen this method of presenting our data in Fig. 1. Drawn in Fig. 1 are the yield envelopes according to the two-parameter criteria and it is seen that of these the best correlation is with the Mohr–Coulomb. It appears also that results for both resins lie on the same yield envelope in normalized stress space. The best fit two-straight lines (also plotted) for resin 1 are consistent with the three-parameter single hexagonal pyramidal criterion [22]:

$$\frac{P_1}{T}+\left(\frac{1}{V}-\frac{1}{T}+\frac{1}{C}\right)P_2-\frac{P_3}{C}=1 \quad (8)$$

where $P_1=P_2=P_3=V$ is the (notional) equi-triaxial tensile yield stress. This relation can be rewritten in terms of a third physically determinable parameter. Choosing this to be the experimentally obtainable equi-biaxial compressive yield stress, $\sigma_{CC}(\sigma_1=0,\ \sigma_2=\sigma_3=\sigma_{CC})$ and defining $|\sigma_{CC}|/|\sigma_C|$ as E, we obtain:

$$\frac{P_1}{T}+\left(\frac{E-C}{EC}\right)P_2-\frac{P_3}{C}=1. \quad (9)$$

For our resins, $C=1$, $T=0.75$, $E=0.92$ (and $V=4.1$). Using these experimental parameters, yield envelopes for plane stress (Fig. 6, $\sigma_2=0$, i.e. (0 1 0) plane of stress space) and shear under pressure (Fig. 3, $\sigma_1+\sigma_3=2\sigma_2$, i.e. $(1\bar{2}1)$ plane) were drawn. Also shown in Fig. 6 are experimental points for resin 1 and another epoxy [30] and published data for materials for which $T \approx 0.75C$: PVC [10, 11], PS [5, 7] and PMMA [9]. It is to be noted that the plane stress yield envelope for fine bands in polystyrene [23] approximates to the pyramidal criteria plotted in Fig. 6. The largest difference between the models is in the biaxial or triaxial tension octants of stress space, where our resin was brittle and failed at much lower stresses when attempts to impose these stress states were made. In fact, resin 1 undergoes a ductile/brittle transition at room temperature in simple tension at strain-rate of $\sim 10^{-4}$ sec^{-1}, as of the ten specimens tested five were brittle and failed at significantly lower stresses. It is, therefore, re-emphasized that in the biaxial and triaxial tension octants, for these resins the yield surface is only notional.

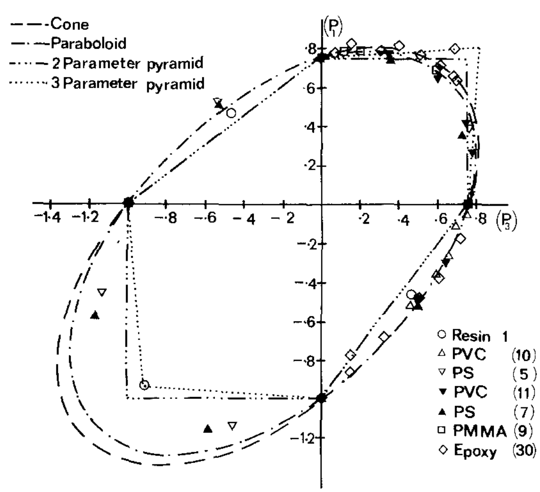

Figure 6 Yield envelopes in the $\sigma_2=0$, i.e. (0 1 0), plane of normalized stress space P_1, P_2, P_3 calculated according to the paraboloidal, conical and two- and three-parameter pyramidal criteria. Data points refer to materials for which $\sigma_T \approx -0.75\,\sigma_C$.

In plane stress the largest difference between the models is in the compression–compression quadrant, where the pyramidal envelopes are the most conservative and the only ones to lie adjacent to our experimental σ_{CC} data. The remainder of the results on all the polymers appears to fit fairly well all the models and, as Raghava *et al.* [14] have pointed out, the plane stress system does not effectively discriminate between the various criteria. The differences between the models become more evident when biaxial or triaxial compression states are investigated, because the yield surfaces are open in triaxial compression and, therefore, tests at high hydrostatic pressures yield critical data. It is seen (Figs. 1 and 2) that the pyramidal criteria are not only the most conservative, but also give the best fit to the experimental data and discrepancies between those and the conical and paraboloidal models become more evident as pressure is increased. In our apparatus higher pressures could not be achieved.

At this stage it is concluded that, for our resins, and quite possibly for other polymers with $T \approx 0.75\ C$, of the simple two-parameter yield criteria the best and most conservative correlation is with the pyramidal [4, 22] but a small improvement results if a three-parameter hexagonal pyramidal surface [22, 23] is postulated with Y of Equation 1 equal to -0.09. It does not appear that when resin 1 became brittle the failure surface was a continuation of the yield surface and thus our criterion refers only to the stressing systems which result in yield prior to failure. It is postulated as a phenomenological correlation and does not depend on a particular model of yielding, as for example, considered by Li and Wu [23]. Further, rather than determine the three material parameters by employing stress concentrations, as they have done, we suggest measuring yield stresses in relatively simple loading systems. We have used as our parameters the tensile, compressive and equibiaxial compressive yield stresses, only the last of which can present some experimental difficulty. To overcome this, plane strain compressive yield stress, σ_{PC}, may be used as the third directly determinable parameter and then Equations 1 to 3, 8 and 9 become:

$$\frac{\sigma_1}{\sigma_T} + \frac{|\sigma_{PC}| - |\sigma_C|}{S\,|\sigma_{PC}|\,|\sigma_C|}\sigma_2 - \frac{\sigma_3}{|\sigma_C|} = 1, \quad (10)$$

where S is a constant, whose value has been suggested to be either 0.5 [28] or the Poisson's ratio, ν [23].

It is not the purpose of this communication to discuss failure mechanisms, but it is to be noted that cracking took place when specimens were extended under superposed pressure even when all the principal stresses were compressive. The surface lips on failure surfaces may be in regions of shear through which cracking is easier. When failure is initiated in the interior of the specimen (e.g. Fig. 5), no hypothesis involving hydraulic fluid penetration of specimen surface flaws can be used to account for cracking normal to a compressive stress. It appears, therefore, that in polymers criteria of failure could be relevantly considered in terms of deviatoric stresses and strains, which is the situation also in ceramics [29].

Acknowledgements
Provision of laboratory facilities by Professor D. Bijl and support by the S.R.C. is appreciated. The work was initiated as an undergraduate project by M.P.

References
1. M. T. HUBER, *Czasopismo Techniczne (Lwów)* **22** (1904) 38.
2. R. VON MISES, *Gottinger Nachrichten, Math-Phys. Klasse* (1913) 582.
3. H. TRESCA, *Comp. Rend. Acad. Sci. Paris* **59** (1864) 754; **64** (1867) 809.
4. I. M. WARD, *J. Mater. Sci.* **6** (1971) 1397.
5. W. WHITNEY and R. D. A. ANDREWS, *J. Polymer Sci. C* **16** (1967) 2981.
6. P. B. BOWDEN and J. A. JUKES, *J. Mater. Sci.* **3** (1968) 183.
7. A. S. ARGON, R. D. ANDREWS, J. A. GODRICK and W. WHITNEY, *J. Appl. Phys.* **39** (1968) 1899.
8. J. R. SAUER, K. D. PAE and S. K. BHATEJA, *J. Macromol. Sci-Phys.* **B8** (1973) 631.
9. S. S. STERNSTEIN, L. ONGCHIN, *Amer. Chem. Soc. Polymer Prepr.* **10** (1969) 1117.
10. J. C. BAUWENS, *J. Polymer. Sci. A2* **8** (1970) 893.
11. R. M. CADDELL, R. S. RAGHAVA and A. G. ATKINS, *Mater. Sci. Eng.* **13** (1974) 113.
12. P. B. BOWDEN and J. A. JUKES, *J. Mater. Sci.* **7** (1972) 52.
13. A. W. CHRISTIANSEN, E. BAER and S. V. RADCLIFFE, *Phil. Mag.* **24** (1971) 451.
14. R. S. RAGHAVA, R. M. CADDELL and G. S. Y. YEH, *J. Mater. Sci.* **8** (1973) 225.
15. N. W. TSCHOEGL, *J. Polymer. Sci. C* **32** (1971) 239.
16. C. A. COULOMB, *Mem. Math. et Phys.* **7** (1773) 343.
17. F. SCHLEISCHER, *Z. Angew. Math. Mech.* **6** (1926) 199.
18. A. MEHLDAHL, *Brown Boveri Rev.* **31** (1944) 260.

19. A. NADAI, "Theory of Flow and Fracture of Solids", Vol. 1 (McGraw-Hill, New York, 1950) p. 207.
20. D. C. DRUCKER, *J. Mech. Phys. Solids* **1** (1953) 217.
21. F. STASSI D'ALIA, *Meccanica* **3** (1967) 178.
22. B. PAUL, "Fracture", Vol. 2, edited by H. H. Liebowitz (Academic Press, New York, 1962) p. 446.
23. J. C. M. Li and J. B. C. WU, *J. Mater. Sci.* **11** (1976) 445.
24. P. B. BOWDEN, "The Physics of Glassy Polymers", edited by R. N. Haward (Applied Science, London, 1973) p. 284.
25. J. J. DIBB, Ph.D. Thesis, University of Bradford (1975).
26. A. S. WRONSKI, Proceedings of the Fourth International Congress on Fracture (Munich, 1973) II-332.
27. C. H. ROBBINS and A. S. WRONSKI, *High Temp. High Press.* **6** (1974) 217.
28. J. G. WILLIAMS and H. FORD, *J. Mech. Eng. Sci.* **6** (1964) 405.
29. M. S. STUCKE and A. S. WRONSKI, *Proc. Brit. Ceram. Soc.* **25** (1975) 109.
30. J. N. SULTAN and F. J. McGARRY, *Polymer Eng. Sci.* **13** (1973) 29.

Received 11 May and accepted 28 May 1976.